Electronic Supplementary Information

Highly selective CO_2 separation from a CO_2/C_2H_2 mixture using a diamine-appended metal-organic framework

Doo San Choi,[a] Dae Won Kim, [a] Dong Won Kang,[a] Minjung Kang, [a] Yun Seok Chae,[a] and Chang Seop Hong*

[a]Department of Chemistry, Korea University, Seoul 02841, Republic of Korea.
E-mail: cshong@korea.ac.kr

Experimental Section

Materials.

Most of the chemicals and solvents used in this experiment were purchased from commercial companies (Sigma Aldrich, Daejung Chemicals, and TCI). All solvents were of reagent grade (≥ 99.0%) and were used without further purification. Ethylenediamine (en, ≥ 98.0%), N-ethylethylenediamine (een, ≥ 98.0%), and N-methylethylenediamine (nmen, ≥ 95.0%) were purchased from Sigma-Aldrich and used without purification. H_4dobpdc (dobpdc^{4-} = 4,4′-dioxido-3,3′-biphenyldicarboxylate) was synthesized according to the previous literature.[1]

Synthesis of Mg_2(dobpdc).

Mg_2(dobpdc) was prepared by a microwave-assisted synthesis from $MgCl_2.6H_2O$ (284.6 mg, 1.400 mmol) and H_4dobpdc (128 mg, 0.467 mmol) in 16 mL of a mixed solvent (DMF/EtOH = 1:1). The mixture was loaded in a 35 mL cell and reacted in a microwave reactor (CEM Discover) for 20 min at 130 °C and 200 psi. After the reaction, the white powder was obtained. The white powder was separated through filtration and washed with DMF and MeOH several times. Mg_2(dobpdc) was dried in vacuum for 6 h.

Synthesis of diamine-Mg_2(dobpdc) (diamine-MOF; diamine = en, nmen, een).

Before the functionalization of diamine, Mg_2(dobpdc) was soaked in MeOH for 1 d at room temperature to replace the DMF molecules coordinated to the open metal sites with the readily removable MeOH. The absence of the C=O stretching vibration of DMF at 1663 cm^{-1} in the IR spectrum suggests the complete removal of DMF from Mg_2(dobpdc) (for IR spectra, please see Figure S1). 100 mg of MeOH-solvated Mg_2(dobpdc) was placed in a 20 mL vial. Excess diamine (50 eq.) was mixed with 10.0 mL of toluene, which was placed in a 20 mL vial containing MeOH-solvated Mg_2(dobpdc). The 20 mL vial was closed with a Teflon cap and sonicated at 60 °C for 3 h. The white powder was separated through filtration and washed with toluene and hexane several times.

Digestion ^{1}H NMR.

Diamine-MOF was activated for 1 h in vacuum at 140 °C using a heating mantle to remove residual diamine from the pores. A sample (5 mg) was mixed with DMSO (0.5 mL) and then two drops of deuterium chloride solution (35 wt. % in D_2O) was added. When the sample became transparent

after about 30 min, it was placed in an NMR tube. Digestion ^{1}H NMR were recorded on Bruker AVANCE III 500 MHz NMR system.

Physical measurements.

IR spectra were obtained using a Nicolet iS10 FT-IR spectrometer. Powder X-ray diffraction (PXRD) patterns were obtained using Cu Kα radiation (λ = 1.5406 Å) on a Rigaku Ultima III diffractometer with a scan speed of 5° min^{-1} and a step size of 0.02°. Thermogravimetric analyses (TGA) were performed with a ramp rate of 2 ^{o}C min^{-1} up to 900 ^{o}C in an N_2 (99.999%) flow using a TA instruments Discovery TGA.

Gas adsorption measurements.

Gas sorptions with CO_2 (99.999%), C_2H_2 (99.999%) and N_2 (99.999%) were performed using a Micromeritics 3flex instrument and ASAP 2020 instrument after the pretreatment of each sample.

Calculations of IAST selectivity and isosteric heats of adsorption.

Gas adsorption isotherms and gas selectivities for CO_2 and C_2H_2 at 293 K were calculated based on the ideal adsorbed solution theory (IAST) proposed by Myers and Prausnitz.[2] In order to predict the sorption performances of Mg_2(dobpdc) and diamine-MOFs for the separation of binary mixed gases, the single-component adsorption isotherms were first fit to a Dual Site Langmuir Freundlich model (DSLF), as below:

$$n(P) = \frac{q_1(k_1P)^{n_1}}{1+(k_1P)^{n_1}} + \frac{q_2(k_2P)^{n_2}}{1+(k_2P)^{n_2}}$$

Where $n(P)$ is the amount of adsorbed gas, P is the equilibrium pressure and q_1, q_2, k_1, k_2, n_1 and n_2 are constants.

The adsorption selectivity, $S_{i,j}$ is defined as :

$$S_{i,j} = \frac{x_i/x_j}{y_i/y_j}$$

where x_i and x_j are the gas uptake capacity at the adsorbed equilibrium of components i and j respectively. The gas molar fractions the i and j components are represented by y_i and y_j, respectively.

The isosteric heat, $Q_{st,}$ is defined as :[3, 4]

$$Q_{st} = RT^2\left(\frac{\partial lnP}{\partial T}\right)$$

The gas adsorption isotherms obtained at 298 and 323 K were fitted by the Dual Site Langmuir Freundlich model (DSLF), respectively.

GCMC simulation.

Grand canonical Monte Carlo (GCMC) simulations were performed for the gas adsorption in the framework and the binding energy calculation by the Sorption module of Material Studio (Accelrys. Materials Studio Getting Started, release 2019).[5] The framework was considered to be rigid, and the optimized C_2H_2 molecules were used. The partial charges for atoms of the framework were derived from QEq method. 2x2x2 unit cells were used during the simulations. The sorption geometries were optimized by Smart algorithm with ultra-fine quality. All parameters for the atoms were modeled with the universal force field (UFF) embedded in the MS modeling package. A cutoff distance of 18.5 Å was used for electrostatic interactions, and the simulation method of the interactions were calculated by using Ewald & Group summation. For each run, the 2×10^5 maximum loading steps, 2×10^7 production steps were employed.

Breakthrough experiments.

The breakthrough curves of a mixed gas of CO_2/C_2H_2 (1:2, v/v) for een-MOF were performed by a BELCAT-II linked with BELMASS mass spectrometer. A fixed-bed column filled with the pelletized samples (425 – 600 μm) was prepared and the total gas flow rate was fixed to total 7 sccm for this measurement (CO_2/C_2H_2/He = 1.5/3.0/2.5). Before breakthrough measurements, all samples were activated at 140 °C for 1 h. All outgas were continuously monitored by the mass spectrometer.[6] In case of the cyclic test, the samples were regenerated at 140 °C for 1 h before each cycle.

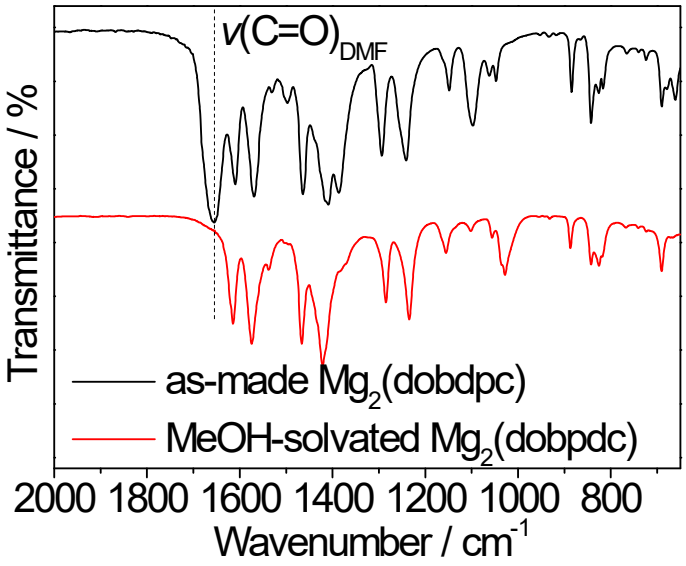

Fig S1. FT-IR data of as-made Mg_2(dobpdc) and MeOH-solvated Mg_2(dobpdc).

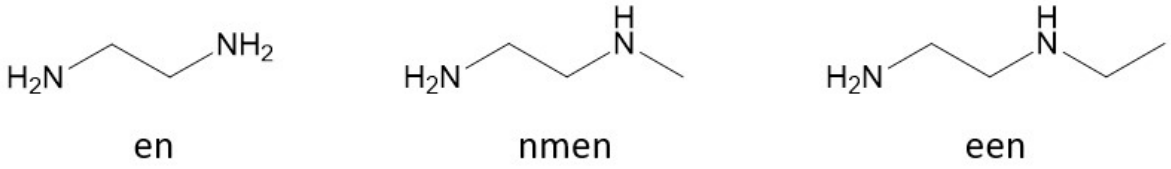

Fig S2. The structure of all diamines used in the experiments.

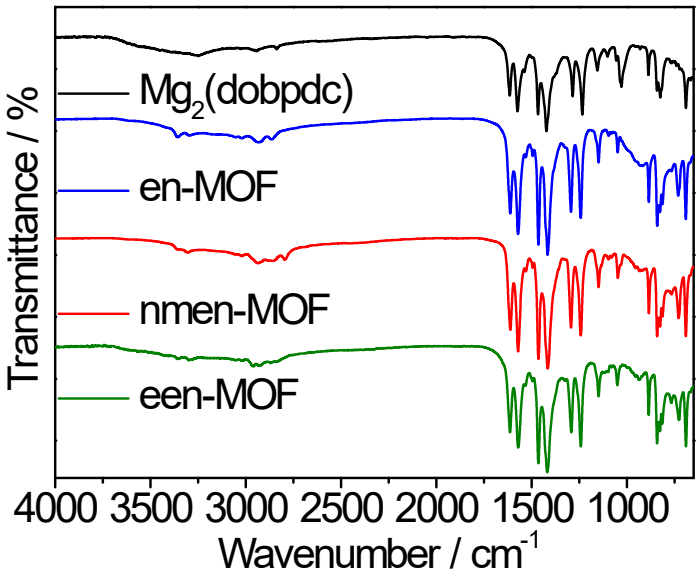

Fig S3. FT-IR data of Mg_2(dobpdc), en-MOF, nmen-MOF, and een-MOF.

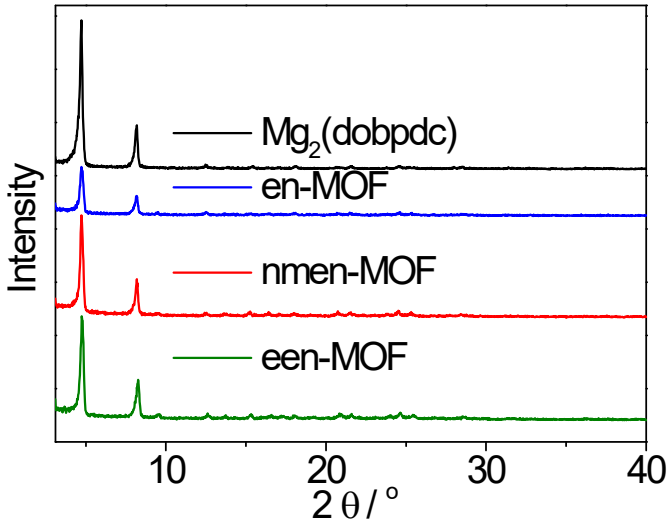

Fig S4. PXRD patterns of Mg_2(dobpdc), en-MOF, nmen-MOF, and een-MOF.

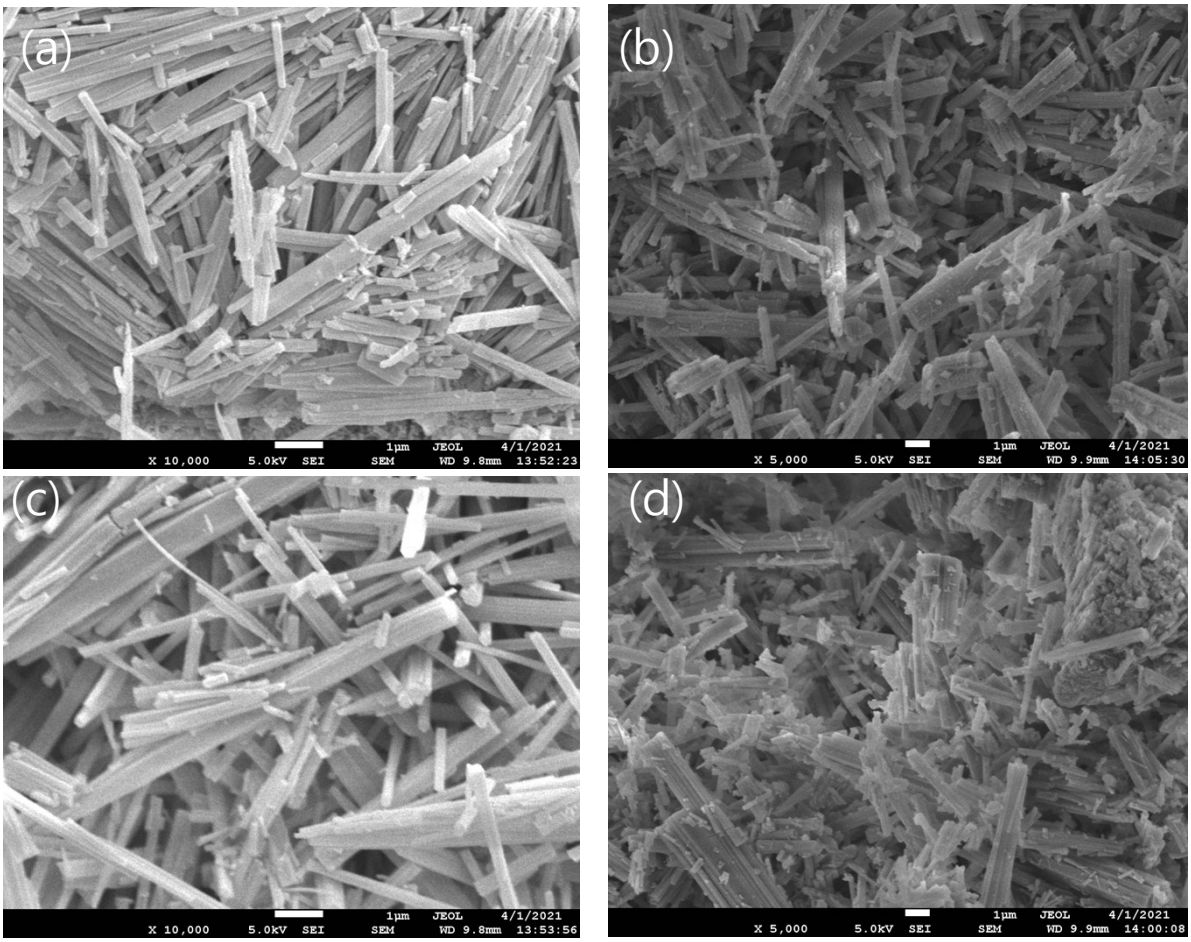

Fig S5. SEM images of (a) Mg_2(dobpdc), (b) en-MOF, (c) nmen-MOF, and (d) een-MOF.

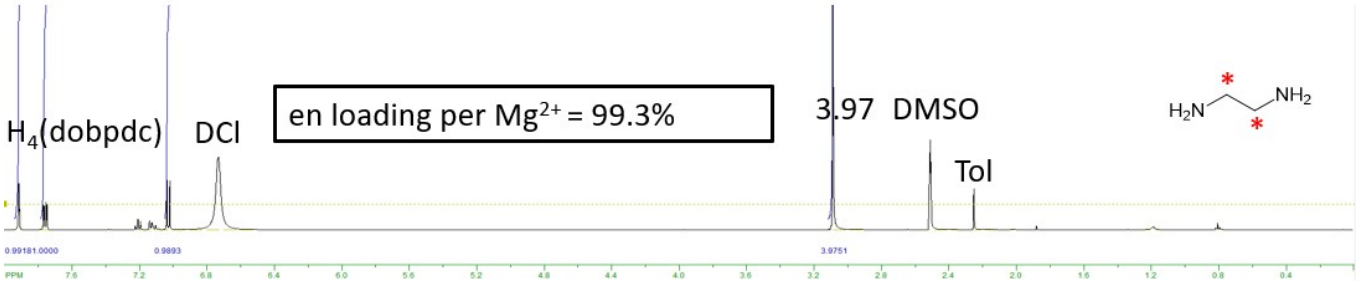

Figure S6. Digestion ^{1}H-NMR of en-MOF.

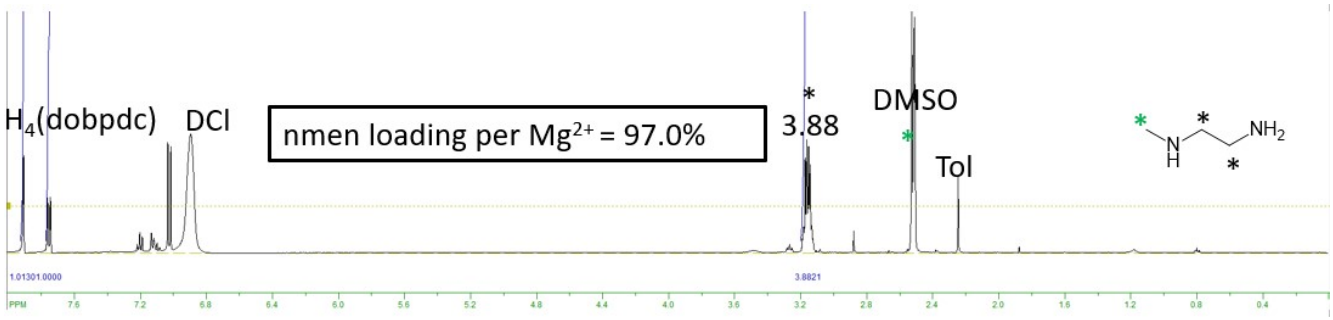

Figure S7. Digestion ^{1}H-NMR of nmen-MOF.

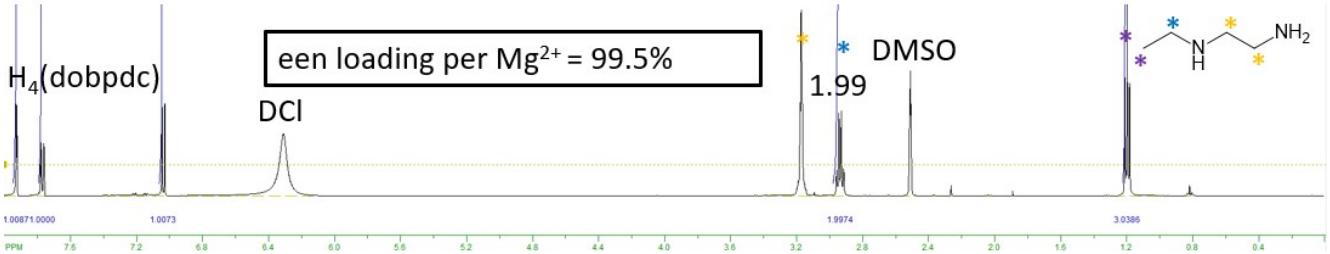

Fig S8. Digestion ^{1}H-NMR of een-MOF.

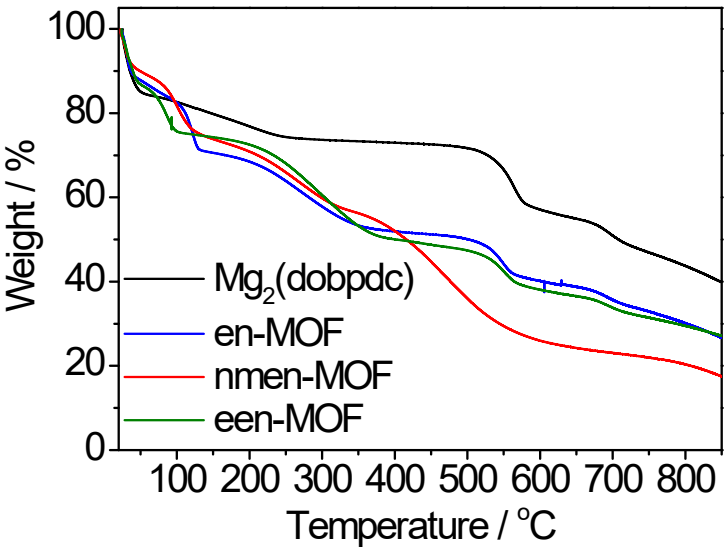

Fig S9. Thermogravimetric analysis of Mg_2(dobpdc), en-MOF, nmen-MOF, and een-MOF.

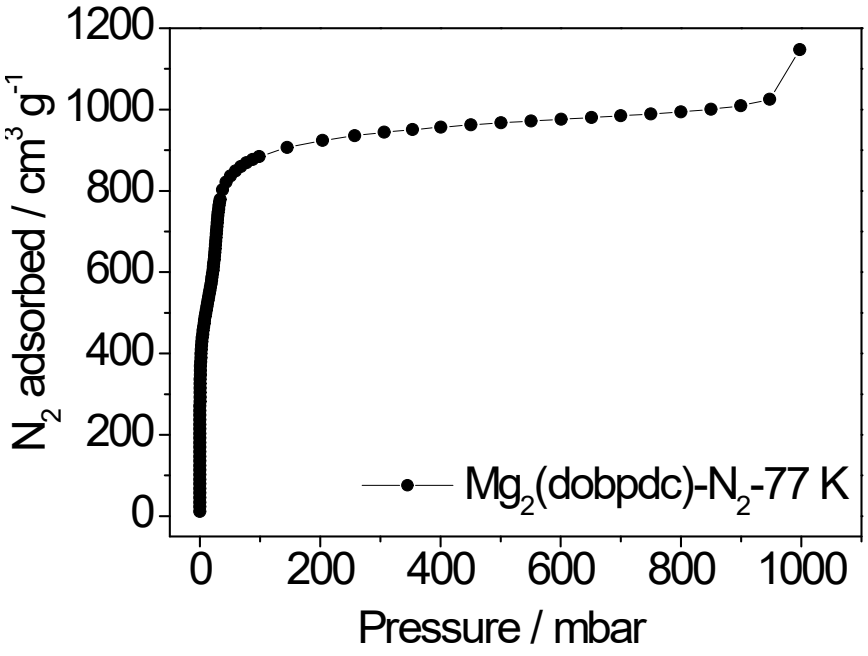

Figure S10. N_2 sorption isotherm for Mg_2(dobpdc) at 77 K.

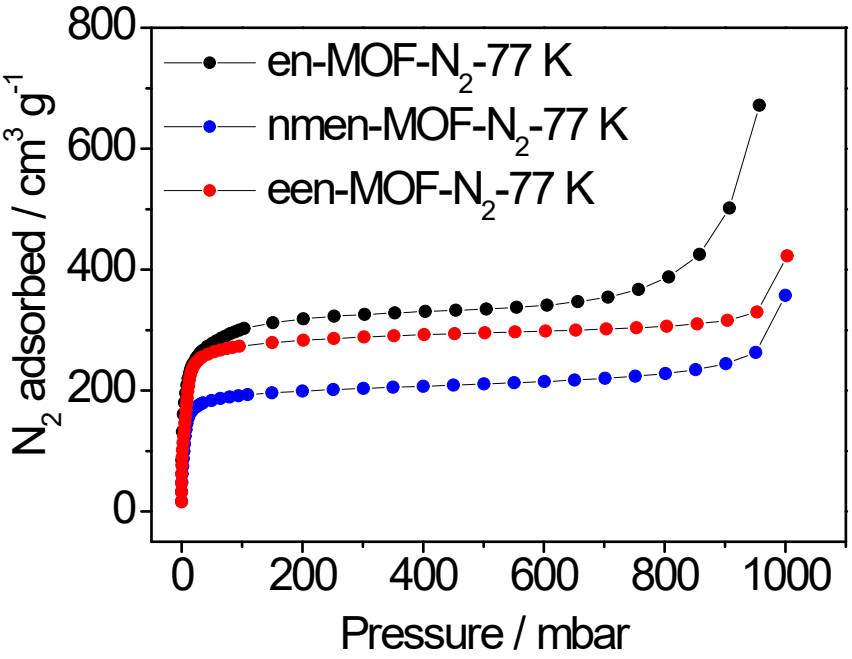

Fig S11. N_2 sorption isotherms for en-MOF, nmen-MOF, and een-MOF at 77 K.

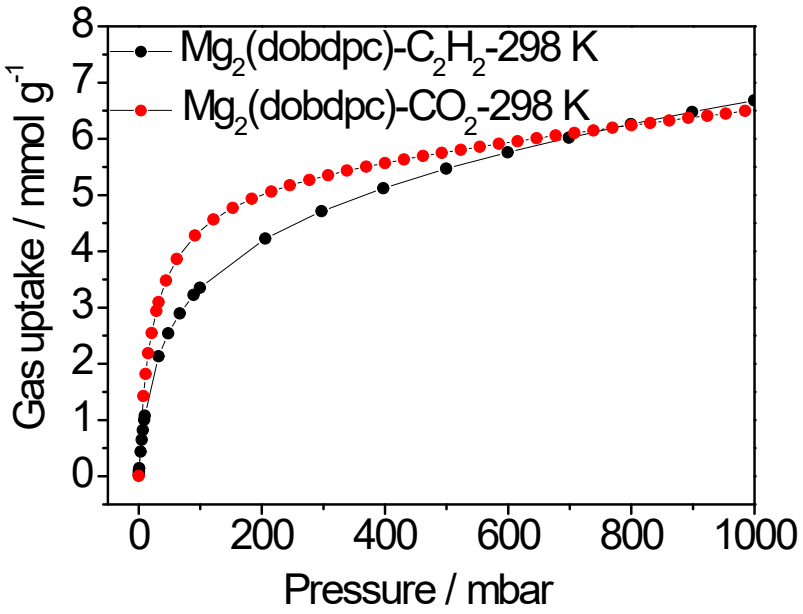

Fig S12. Experimental CO_2 and C_2H_2 sorption isotherms for Mg_2(dobpdc) at 298 K.

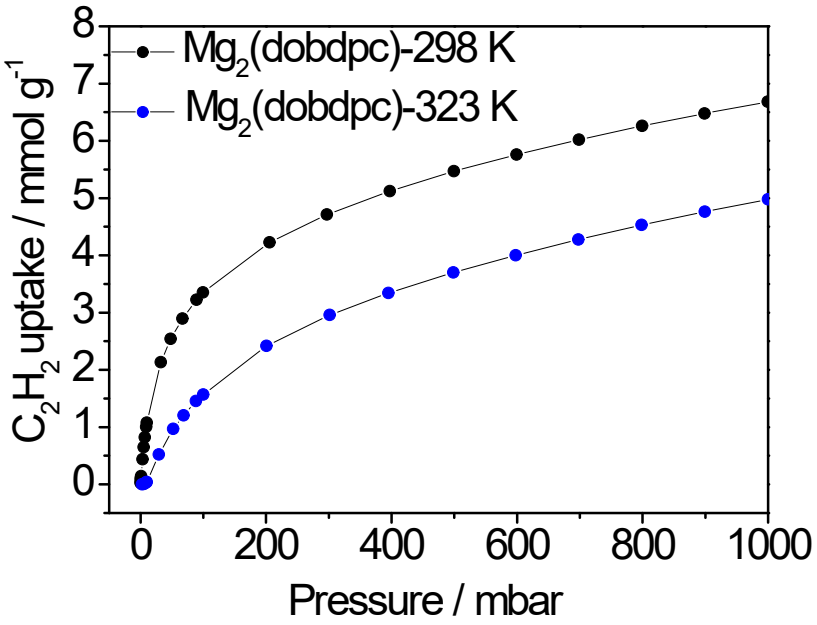

Fig S13. Experimental C_2H_2 sorption isotherms for Mg_2(dobpdc) at the indicated temperatures.

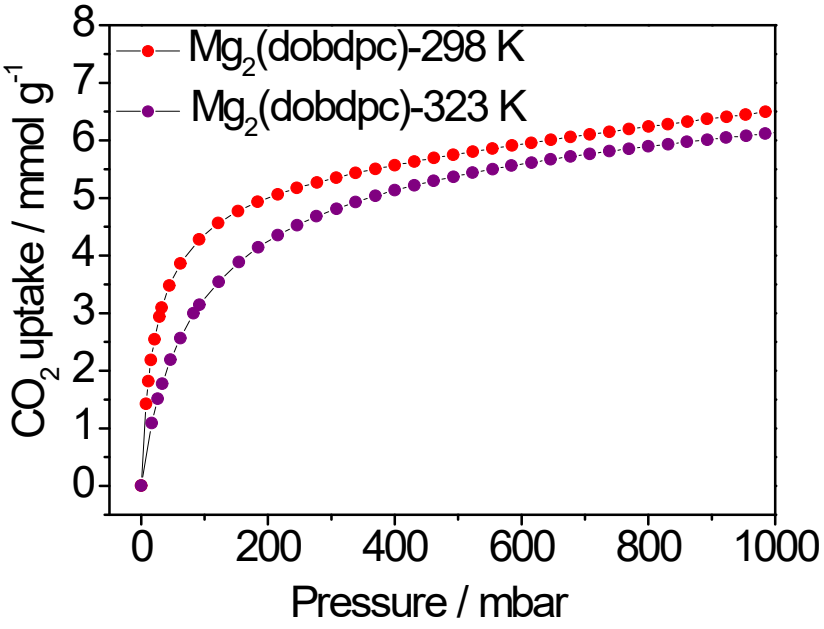

Fig S14. Experimental CO_2 sorption isotherms for Mg_2(dobpdc) at the indicated temperatures.

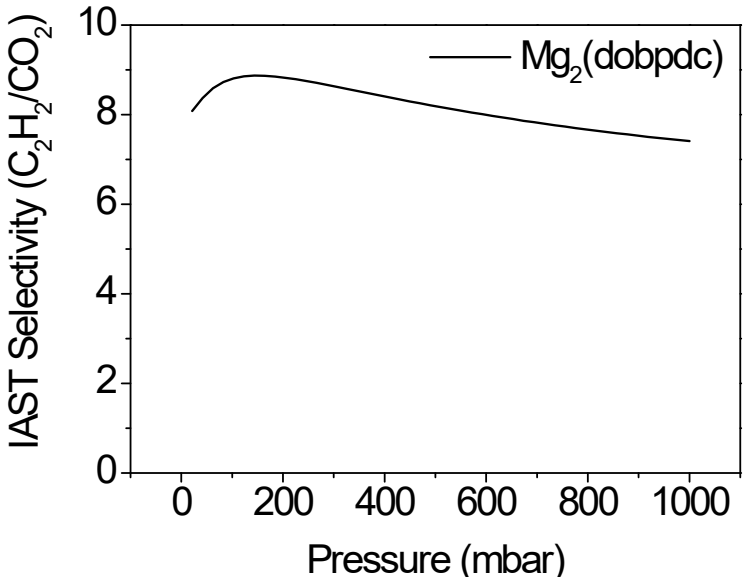

Fig S15. Calculated C_2H_2 /CO_2 (2/1, v/v) IAST selectivity for Mg_2(dobpdc) at 298 K.

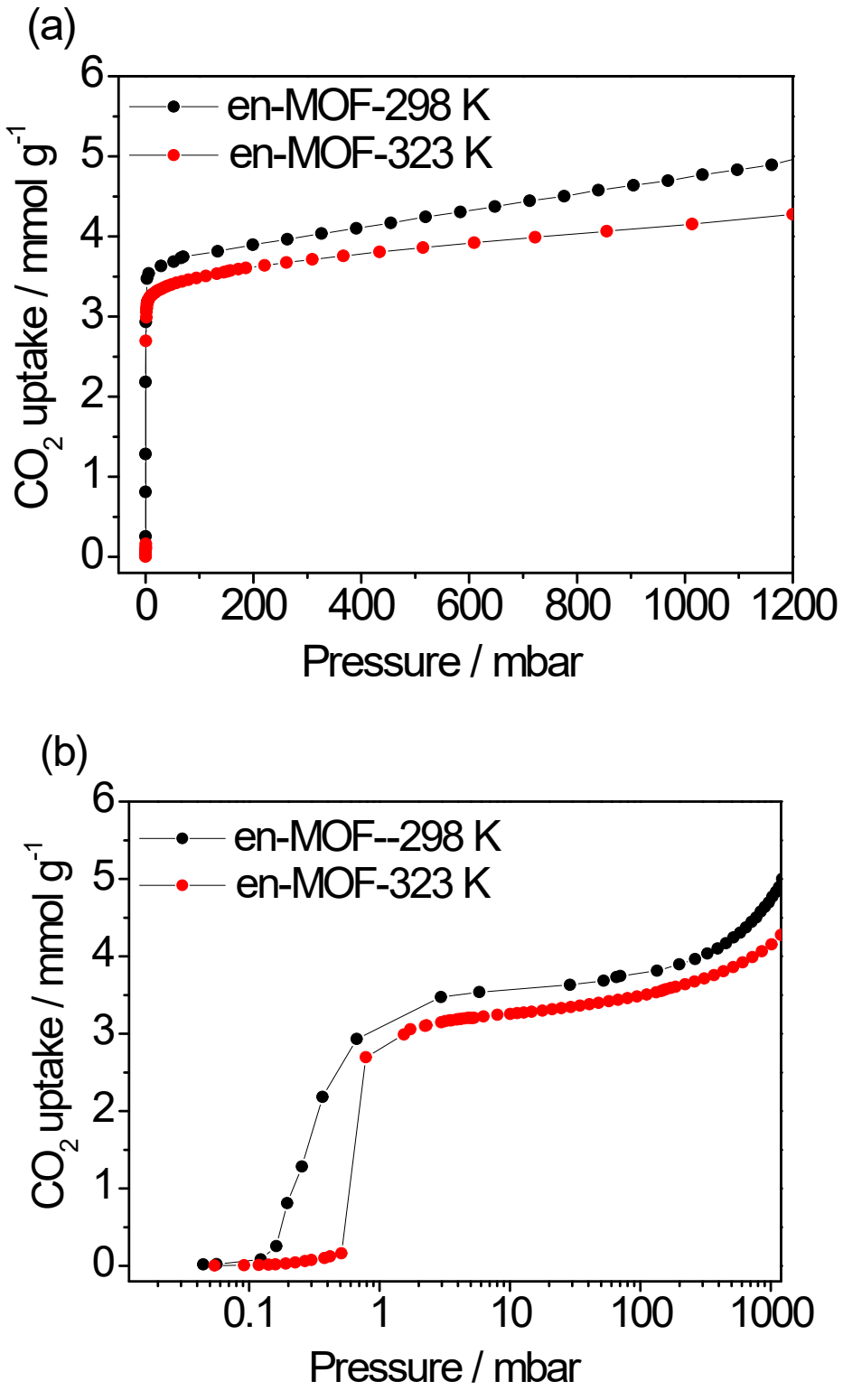

Fig S16. (a) Adsorption isotherms of CO_2 for en-MOF at the indicated temperatures. (b) Logarithmic-scale plot of (a).

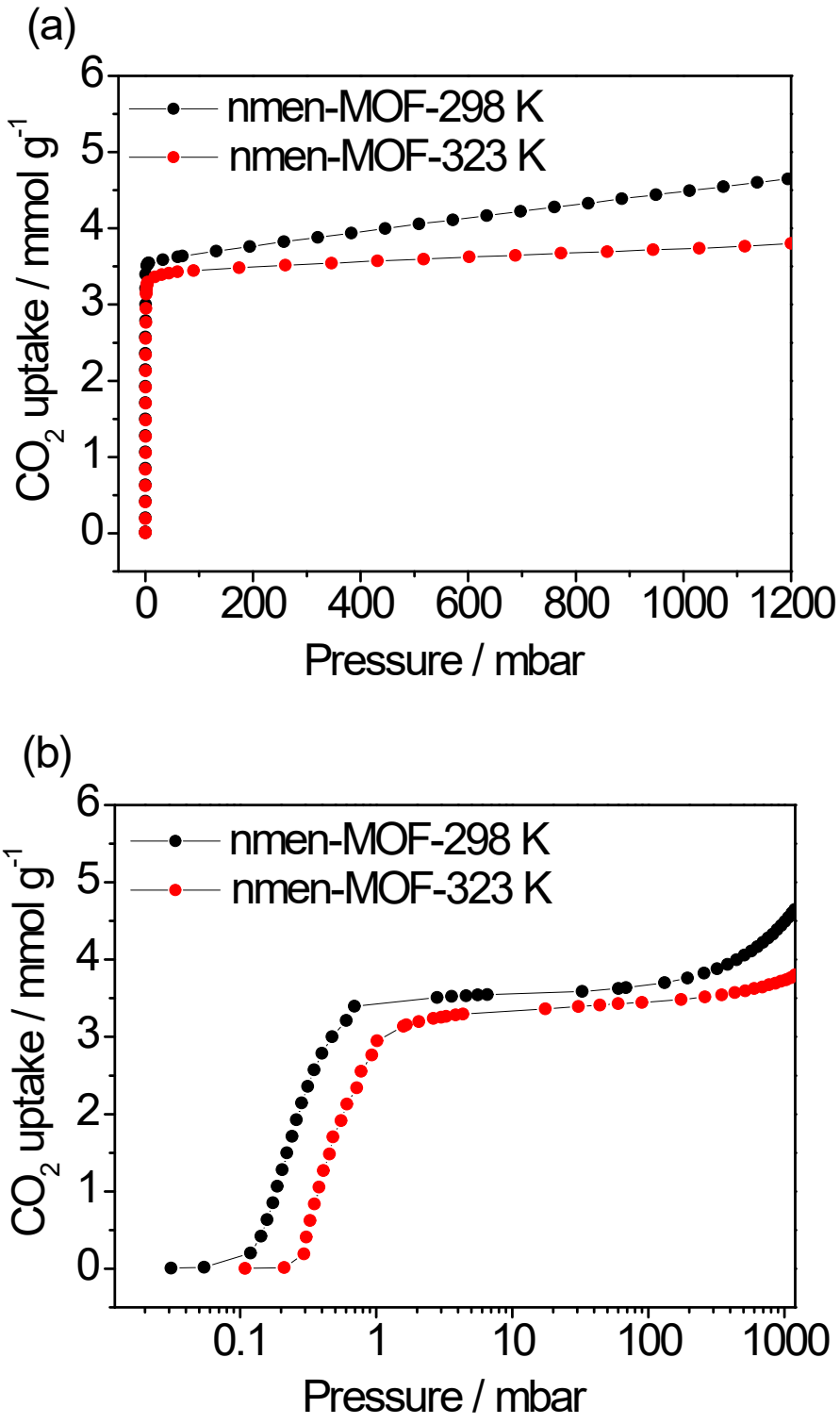

Fig S17. (a) Adsorption isotherms of CO_2 for nmen-MOF at the indicated temperatures. (b) Logarithmic-scale plot of (a).

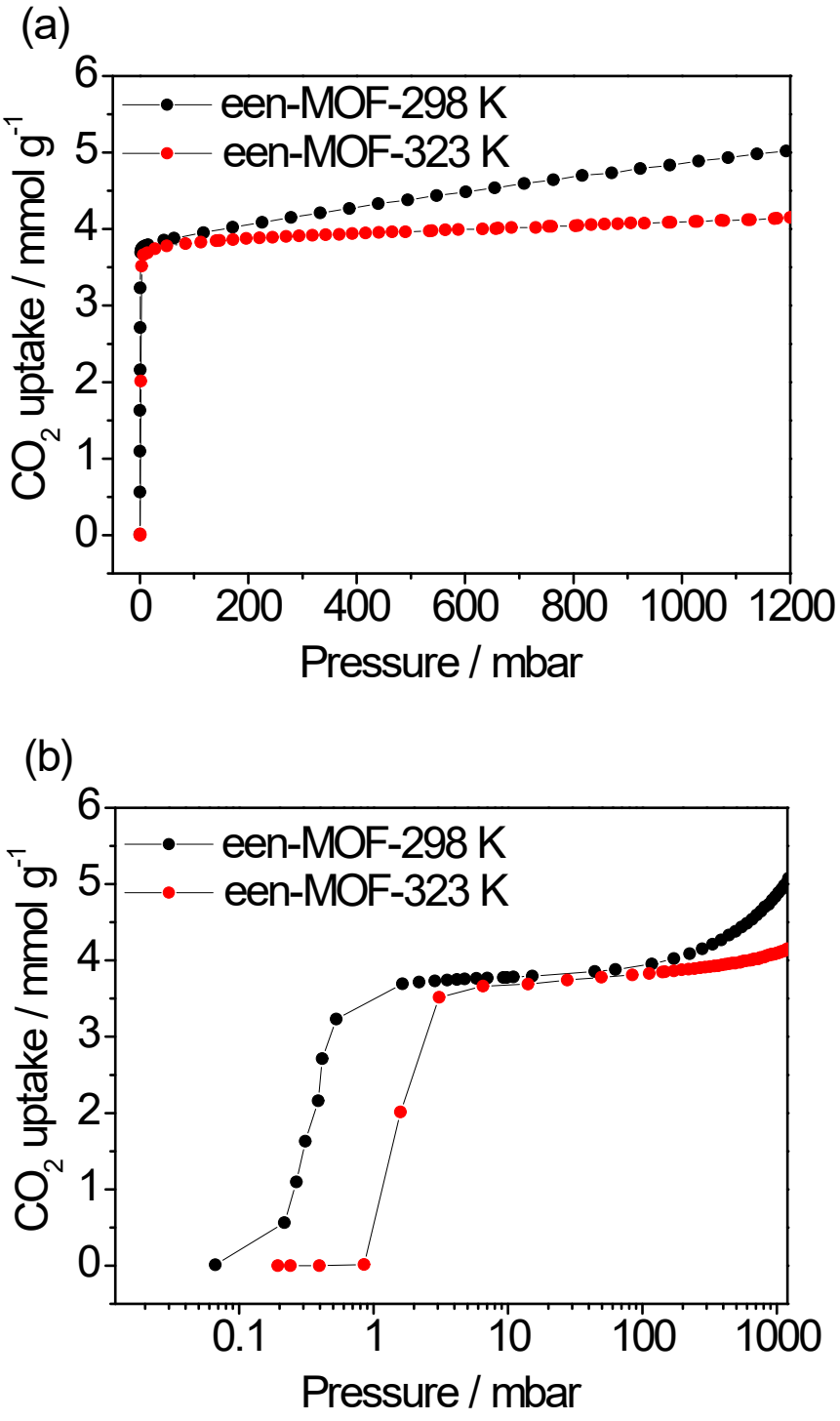

Fig S18. (a) Adsorption isotherms of CO_2 for een-MOF at the indicated temperatures. (b) Logarithmic-scale plot of (a).

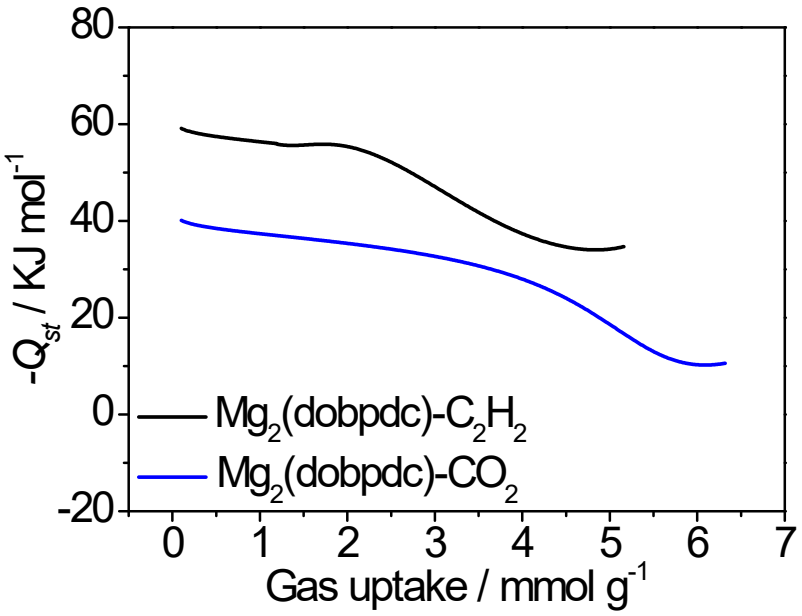

Fig S19. Isosteric heats of adsorption of C_2H_2 and CO_2 for Mg_2(dobpdc).

Table S1. -Q_{st} value of CO_2 and C_2H_2 for reported materials.

Materials	-Q_{st} of CO_2 (KJ / mol)	-Q_{st} of C_2H_2 (KJ / mol)	Ref.
Mn(bdc)(dpe)	29.5	27.8	[7]
SIFSIX-3-Ni	51	36.5	[8]
CD-MOF-1	41	17	[9]
CD-MOF-2	67.5	25	[9]
$Tm_2(OH\text{-}bdc)_2(\mu_3\text{-}OH)_2$	32.7	26.0	[10]
MUF-16	32	25.8	[11]
PCP-NH_2-ipa	36.6	26.8	[12]
PCP-NH_2-bdc	34.57	25.6	[12]
Cd-NP	27.7	NA	[13]
Fe-MOF-74	30	45	[14]
Mg_2(dobpdc)	40.1	59.1	This work
en-MOF	71.2	22.3	This work
nmen-MOF	62.32	23.9	This work
een-MOF	68.77	23.4	This work

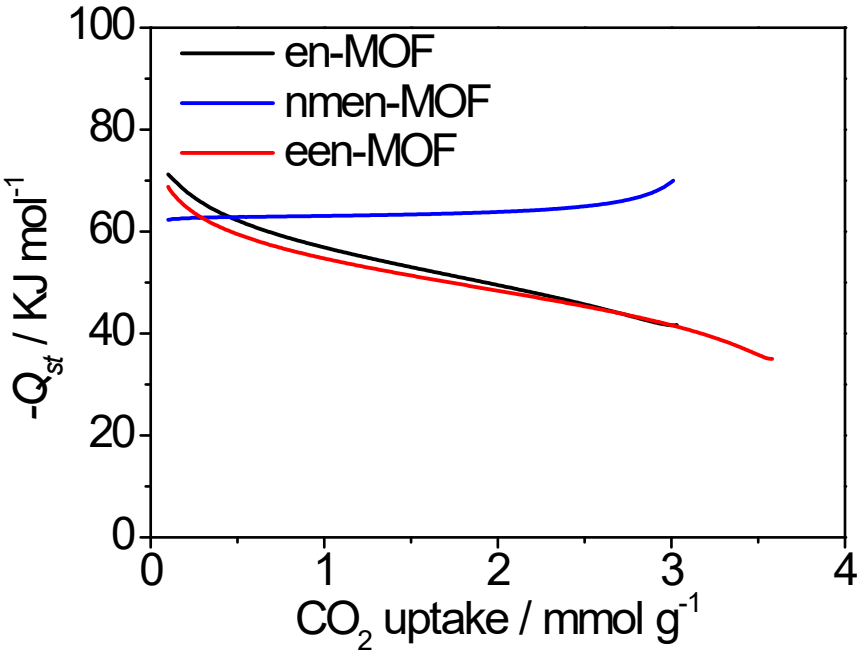

Fig S20. Isosteric heats of adsorption of CO_2 for en-MOF, nmen-MOF, and een-MOF.

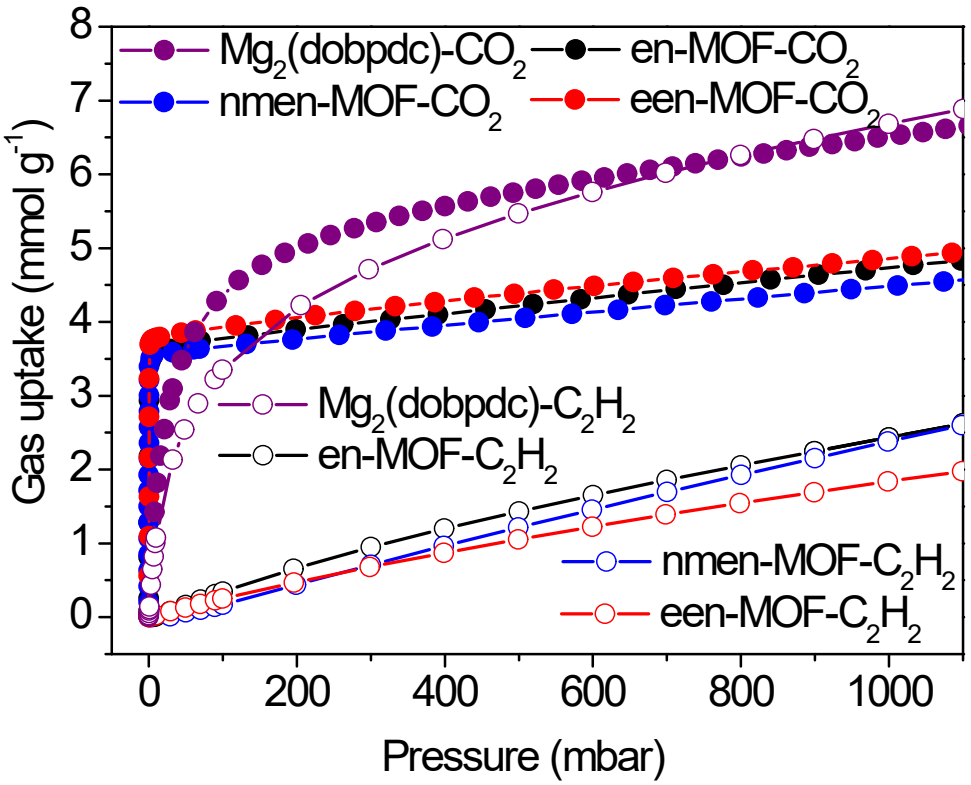

Fig S21. Adsorption isotherms of CO_2 and C_2H_2 for Mg_2(dobpdc), en-MOF, nmen-MOF, and een-MOF at 298 K.

Table S2. Comparison of CO_2 and C_2H_2 uptake of CO_2/C_2H_2 for reported materials. CO_2 and C_2H_2 adsorption values at 30 mbar were extracted from these references using a WebPlotDigitizer.

Materials	T(K)	CO_2 uptake[a]	C_2H_2 uptake[b]	Ref.
Mn(bdc)(dpe)	273	0.22/2.09	0.32	[7]
SIFSIX-3-Ni	298	2.25/2.70	3.30	[8]
CD-MOF-1	298	1.1/2.87	2.23	[9]
CD-MOF-2	298	1.3/2.65	2.03	[9]
$Tm_2(OH\text{-}bdc)_2(\mu_3\text{-}OH)_2$	298	1.35/5.83	2.10	[10]
MUF-16	293	0.49/2.14	0.18	[11]
PCP-NH_2-ipa	298	0.80/3.21	1.93	[12]
PCP-NH_2-bdc	298	0.75/3.03	1.90	[12]
Cd-NP	298	0.36/2.59	0.43	[13]
en-MOF	298	3.64/4.48	2.43	This work
nmen-MOF	298	3.58/4.73	2.38	This work
een-MOF	298	3.82/4.85	1.84	This work

[a]Gravimetric uptake (mmol g^{-1}) at 30 mbar/1000 mbar, except Mn(bdc)(dpe) at 30 mbar/91 mbar.
[b]Gravimetric uptake (mmol g^{-1}) at 1000 mbar, except Mn(bdc)(dpe) at 91 mbar.

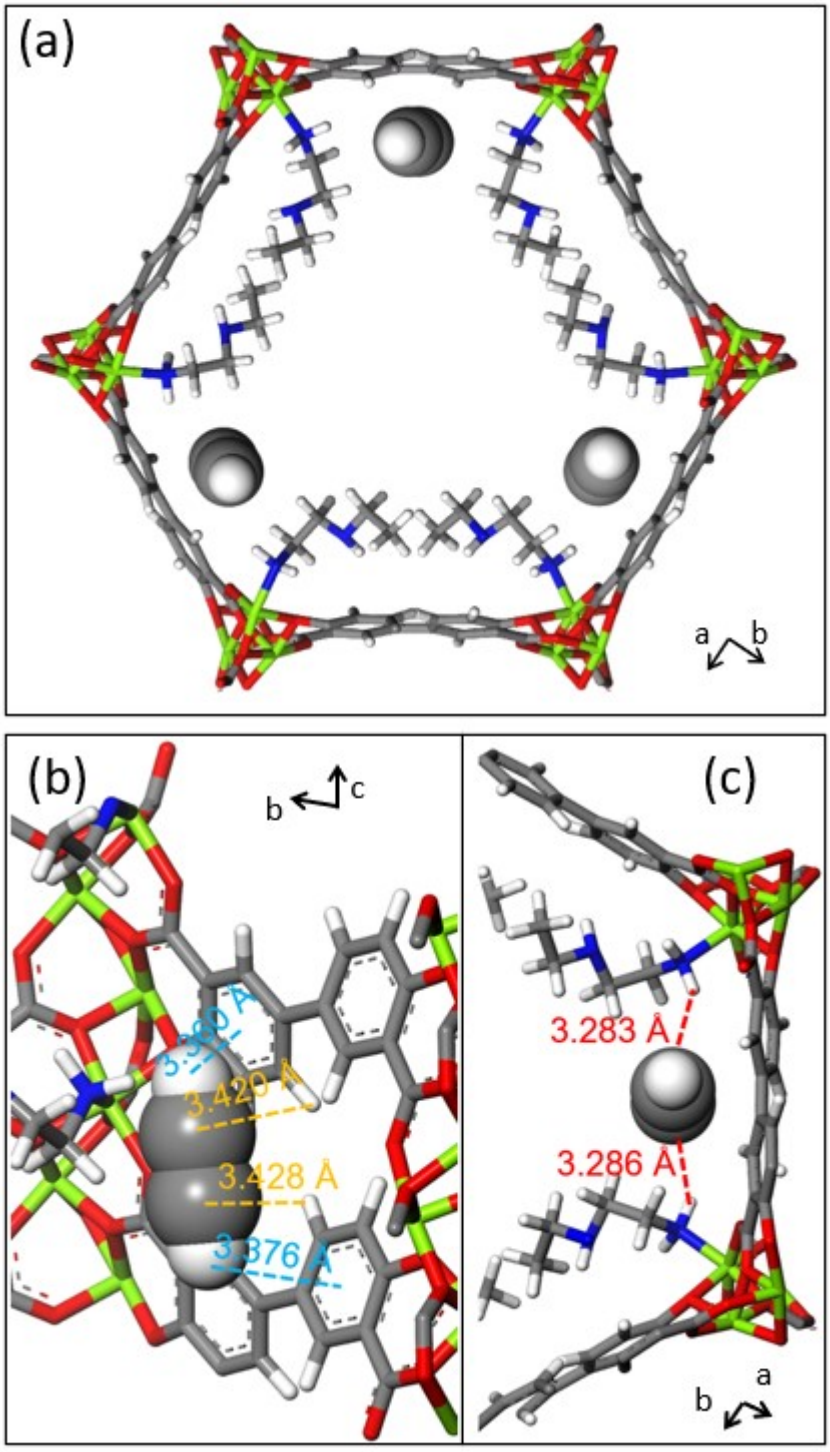

Fig S22. Grand canonical Monte Carlo (GCMC) simulations of C_2H_2 adsorption in een-MOF. (a) View of the C_2H_2 binding sites (C_2H_2 molecules in space-filling mode) in een-MOF. (b) Interaction between C_2H_2 and the ligand dobpdc^{4-}. Blue and orange dotted lines represent the interactions between H of C_2H_2 and the centriod of a phenyl ring, and the interactions between C of C_2H_2 and H of the phenyl ring, respectively. (c) Interaction between C_2H_2 and een groups. Red dotted lines represent the interaction between C of C_2H_2 and H of een.

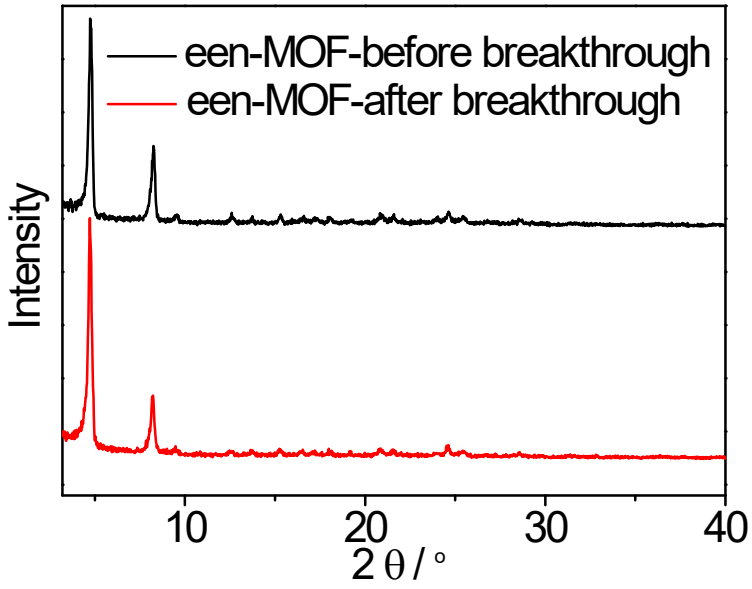

Fig S23. PXRD patterns of een-MOF before and after breakthrough experiments. een-MOF was regenerated at 140 °C for 1 h.

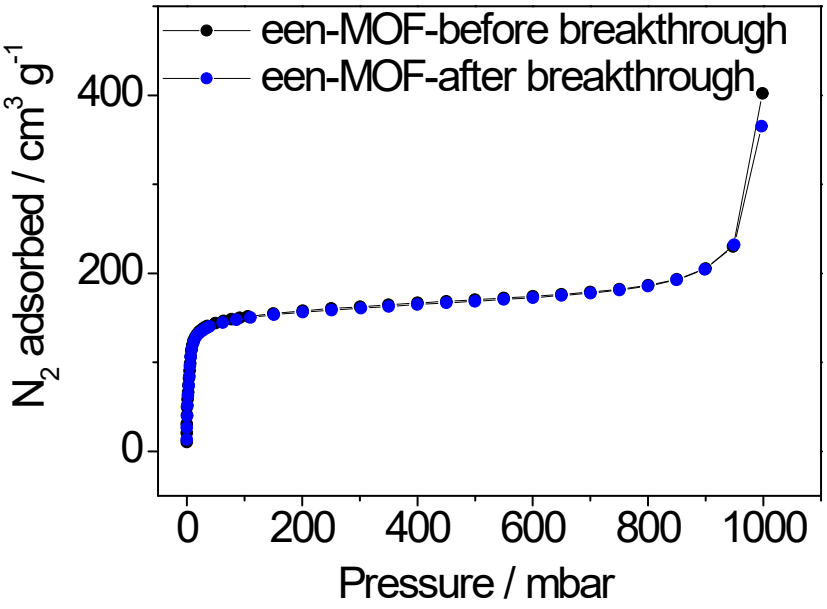

Fig S24. N_2 sorption isotherms for een-MOF before and after breakthrough experiments. een-MOF was regenerated at 140 °C for 1 h.

References

1. T. M. McDonald, W. R. Lee, J. A. Mason, B. M. Wiers, C. S. Hong and J. R. Long, *J. Am. Chem. Soc.*, 2012, **134**, 7056-7065.
2. A. L. Myers and J. M. Prausnitz, *AIChE J*, 1965, **11**, 121-127.
3. L. Zhang, K. Jiang, Y. Yang, Y. Cui, B. Chen and G. Qian, *J. Solid State Chem.*, 2017, **255**, 102-107.
4. H. Pan, J. A. Ritter and P. B. Balbuena, *Langmuir*, 1998, **14**, 6323-6327.
5. , Sorption Module - Accelrys Inc. San Diego, 2011.
6. D. W. Kang, M. Kang, D. W. Kim, H. Kim, Y. H. Lee, H. Yun, J. H. Choe and C. S. Hong, *Adv. Sustainable Syst.*, 2020, **5**, 2000161.
7. M. L. Foo, R. Matsuda, Y. Hijikata, R. Krishna, H. Sato, S. Horike, A. Hori, J. Duan, Y. Sato, Y. Kubota, M. Takata and S. Kitagawa, *J. Am. Chem. Soc.*, 2016, **138**, 3022-3030.
8. K.-J. Chen, Hayley S. Scott, David G. Madden, T. Pham, A. Kumar, A. Bajpai, M. Lusi, Katherine A. Forrest, B. Space, John J. Perry and Michael J. Zaworotko, *Chem*, 2016, **1**, 753-765.
9. L. Li, J. Wang, Z. Zhang, Q. Yang, Y. Yang, B. Su, Z. Bao and Q. Ren, *ACS Appl. Mater. Interfaces*, 2019, **11**, 2543-2550.
10. D. Ma, Z. Li, J. Zhu, Y. Zhou, L. Chen, X. Mai, M. Liufu, Y. Wu and Y. Li, *J. Mater. Chem. A*, 2020, **8**, 11933-11937.
11. O. T. Qazvini, R. Babarao and S. G. Telfer, *Nat. Commun.*, 2021, **12**, 197.
12. Y. Gu, J. J. Zheng, K. I. Otake, M. Shivanna, S. Sakaki, H. Yoshino, M. Ohba, S. Kawaguchi, Y. Wang, F. Li and S. Kitagawa, *Angew. Chem. Int. Ed.*, 2021, **60**, 11688-11694.
13. Y. Xie, H. Cui, H. Wu, R. B. Lin, W. Zhou and B. Chen, *Angew. Chem. Int. Ed.*, 2021, **60**, 9604-9609.
14. A. Luna-Triguero, J. M. Vicent-Luna, R. M. Madero-Castro, P. Gomez-Alvarez and S. Calero, *ACS Appl. Mater. Interfaces*, 2019, **11**, 31499-31507.